PPS
Paper
www.rsc.org/pps

Fluorescence kinetics of aqueous solutions of tetracycline and its complexes with Mg^{2+} and Ca^{2+} †

Siegfried Schneider,*[a] Matthias O. Schmitt,[a] Georg Brehm,[a] Markus Reiher,[a] Pavel Matousek[b] and Mike Towrie[b]

[a] *Institut für Physikalische und Theoretische Chemie, Friedrich-Alexander-Universität Erlangen-Nürnberg, D-91058 Erlangen, Germany. E-mail: Schneider@chemie.uni-erlangen.de*
[b] *Central Laser Facility, CCLRC Rutherford Appleton Laboratory, Chilton, Didcot, Oxfordshire, UK OX11 0QX. E-mail: P.Matousek@rl.ac.uk*

Received 24th April 2003, Accepted 17th July 2003
First published as an Advance Article on the web 6th August 2003

The fluorescence spectra of acidified aqueous solutions of tetracycline (tcH_3^+) exhibit three components with slightly different degrees of anisotropy: the 'blue' component ($\lambda_d \approx 475$ nm) decays on the timescale of a few picoseconds; the second, most intense component ($\lambda_d \approx 530$ nm) shows decay times of about 25 (H_3O^+) and 70 ps (D_3O^+); the third component ($\lambda_d \approx 650$ nm) is longer lived ($\tau \approx 200$ ps). All three fluorescence components appear quasi-instantaneously, thus providing evidence that the relaxation processes which give rise to the unusually large Stokes shifts occur on a (sub-)picosecond timescale. The effect of H/D exchange suggests that these relaxation processes involve excited-state intramolecular proton transfer (ESIPT) of OH10 and/or OH12, but does not exclude a change in the hydrogen-bonding pattern to the solvent molecules. The low overall fluorescence yield of the fully protonated form must be correlated to the presence of a very fast decaying species. In alkaline aqueous solution, the fluorescence of the dianion (tc^{2-}) essentially comprises two components; the decay time of the stronger, shorter-lived component is about 30 ps, that of the weaker, longer-lived one about 160 ps. The relative amplitude of the latter is larger at pH 11 than at pH 8.5, in accordance with the increase in the steady-state fluorescence intensity upon increasing the pH from 8.5 to 11. Complexation of the dianion with divalent metal ions like Mg^{2+} or Ca^{2+} leads to a strong enhancement of the steady-state fluorescence. In the time-resolved spectra, the decay time of the major fluorescence component exhibits approximately a five-fold increase in comparison to the major component of the dianion. It is about 150 ps in both types of complexes. The decay times of the minor component are increased to about 500 (Mg^{2+}) and 320 ps (Ca^{2+}). The absence of the ultra-fast component in the fluorescence of the dianion and its metal complexes provides evidence that a reaction of OH12 must be responsible for the ultra-fast fluorescence component in tcH_3^+. The existence of a component with a lifetime of several tens of picoseconds in all samples suggests the involvement of hydrogen bonding at OH10 during the formation of the emitting species. DFT calculations for the isolated molecule provide evidence that ESIPT is indeed an energetically allowed relaxation process for those isomers that have only one intramolecular hydrogen bond to O11. The ESIPT process yields primary photoproducts that should emit at much longer wavelengths, thereby explaining the unusually large fluorescence Stokes shift.

1 Introduction

Since the discovery of their antibiotic action in 1947, tetracycline and several of its derivatives have been widely applied.[1,2] Besides new applications, *e.g.* as inhibitors of metalloproteinase activity,[3] tetracyclines have attracted much interest in the field of tetracycline-dependent gene regulation.[4–7] In the wild-type Tet repressor system, which is operative in the Tn10 encoded resistance mechanism of Gram-negative bacteria against tetracylines, the regulator protein TetR binds to the corresponding operator tetO on the DNA.[4,5] In this way, TetR prevents transcription of the genes controlling the synthesis of further TetR and of the membrane-bound antiporter protein TetA. If tetracyclines penetrate through the cell wall, they are, as complexes with divalent metal ions, bound with a very high association constant in the binding pockets of TetR. As a consequence, allosteric changes are induced in the DNA binding domain and TetR is released from the DNA, thereby allowing its transcription.

One common procedure to determine these association constants is by means of fluorescence titration.[8] This technique works generally both for the determination of complexation constants between tetracyclines and selected divalent metal ions and the binding of the tetracycline/metal ion complex in the homodimeric TetR protein. The main reason for the effectiveness of fluorescence titration is the phenomenological observation that the fluorescence yield of the tetracycline/metal ion complexes is higher than that of metal-free tetracyclines by about a factor of 5 and that incorporation into the binding pocket of TetR results in a further increase of the fluorescence yield by about a factor of 30. The reasons for these fluorescence enhancements are by no means understood. To the best of our knowledge, no systematic study of the fluorescence kinetics of tetracyclines has been published up to now.

It could be speculated that intra- and intermolecular hydrogen bonding is a decisive factor because it causes highly effective radiationless relaxation processes, hence, we have recorded time-resolved fluorescence spectra of tetracycline and several derivatives under different experimental conditions. The solvents employed were H_2O, D_2O and H_2O/MeOH mixtures. The pH (pD) was varied between 2 (fully protonated form) and 11 (completely deprotonated form). Since the degree of protonation of the complexes with metal ions is uniquely determined at high pH only, the investigations of complexes were restricted to basic solutions.

† This paper is dedicated to Professor Fred Lewis on the event of his 60th birthday.

 DOI: 10.1039/b304523b

2 Materials and methods

2.1 Materials

The chemical structure and the numbering of atoms of protonated tetracycline (tcH_3^+) are shown in Scheme 1. The commercially available compound (tetracycline hydrochloride, Fluka, Germany) was dissolved in H_2O (D_2O) and either HCl (DCl) or NaOH (NaOD) were added until the desired pH (pD) was established.

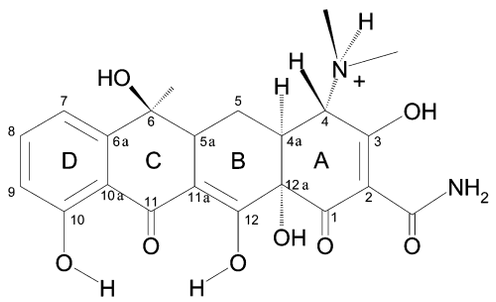

Scheme 1 Chemical structure of fully protonated tetracycline and numbering of the atoms. Note that several alternative tautomeric and rotameric forms could exist in solution.

For the investigation of the metal ion complexes, stock solutions of $MgCl_2$ and $CaCl_2$ were prepared in H_2O (D_2O) and added to the alkaline solutions until the ratio of tetracycline to metal ion approached 1.

Alternatively, appropriate amounts of MeOH (MeOD) were added to the aqueous solutions in order to study the effect of intermolecular hydrogen bonding on excited-state lifetimes.

2.2 Spectroscopy

Steady-state fluorescence emission spectra and the degree of anisotropy were recorded by means of a Jobin Yvon Fluoromax-3 instrument, employing solutions in thermostated 1 cm × 1 cm quartz cuvettes.

A newly developed experimental set-up employing a fast Kerr gate was used for monitoring the time-resolved fluorescence spectra. The molecules are excited at 266 nm by the third harmonic of the amplified output of a mode-locked Ti:sapphire laser ($t_p \approx 100$ fs, repetition rate ~1 KHz). The fluorescence, which is collected at 90° to the excitation beam with the polarization at the magic angle, passes through two crossed polarizers, with a cell containing the Kerr medium (CS_2) in between. The fundamental output of the system at 800 nm is focused into the Kerr cell after proper delay and acts as gating pulse. As a consequence, only that part of the fluorescence emitted within the opening 4 ps window passes through the Kerr gate. After dispersion by a spectrograph, the spectral distribution of the fluorescence is monitored by means of a CCD camera. (For more details, see ref. 9 and 10.) The displayed spectra are not corrected for the pixel and wavelength-dependent detection efficiency. Therefore, the intensity modulations seen are not vibronic structures, but instrumental artifacts.

Since the sample solutions are flowed in an open jet, one cannot exclude fluorescence quenching by dissolved oxygen as an unwanted side effect, at least for those components that exhibit a decay time of more than 500 ps.

2.3 Quantum chemical methodology

All quantum chemical calculations were carried out with the density functional programs provided by the Turbomole 5.1 and 5.6 suites of programs.[11] Since we aimed at a good description of excited-state energies within density functional theory (DFT), we used the B3LYP hybrid functional,[12,13] which is known to perform best when compared to other standard density functionals.[14] All excitation energies were calculated within the time-dependent DFT (TDDFT) framework described in ref. 15 and 16. Structure optimization in the first excited singlet state was performed by using the method very recently developed by Furche and Ahlrichs.[17] The TZVP basis set developed by Ahlrichs and co-workers was employed for all atoms in all calculations.[18] TDDFT test calculations with Ahlrichs' TZVPP basis set yielded excitation energies close to those from TZVP calculations. Therefore, the sufficiently large, but computationally more efficient, TZVP basis set was used throughout.

In order to assess the effect of solvation of the tetracycline molecules, we also studied isolated complexes of tetracycline with six water molecules arranged initially as in the crystal. Upon structure optimization, these water molecules changed their position depending on the isomeric form chosen. Therefore, absolute values provided by these calculations cannot be used for a quantitative discussion. However, they give an estimate of the effect of solvation on excitation energies.

For the calculation of intramolecular hydrogen-bond energies we utilized the SEN approach described in ref. 19, where a linear relationship between the shared-electron number of two atoms and their interaction energy is stipulated.

3 Results

3.1 Steady-state absorption and fluorescence measurements

The UV/vis absorption spectra of tetracyclines are generally discussed as superposition of the contributions of two separated chromophores:[20–23] one is the so-called A chromophore, which comprises a tricarbonylmethane keto-enol system spanning from C1 to C3, including the substituents (O1, carboxamide group at C2 and OH3); the second, usually termed the BCD chromophore, comprises the π-electron system located on rings B, C and D (see Scheme 1). The BCD chromophore causes the first absorption band around 380 nm [Fig. 1(A)]. Below 320 nm, both chromophores contribute to the observed absorption. At low pH, the tetracyclines are fully protonated, as shown in Scheme 1. At increased pH, the proton at O3 is released and a zwitterion is formed ($pK_{a1} = 3.3$, Scheme 2). Accordingly, the major changes in the UV/vis absorption spectrum are found below 350 nm.[21–23] An increase of the pH above pK_{a2} (7.7) causes the dissociation of the proton at O12, which manifests itself in a bathochromic shift of the first absorption band by about 20 nm. The release of the proton at N4 ($pK_{a3} \approx 9.5$) induces changes in the absorption spectra below 350 nm (A-chromophore contribution), but also in the red absorption band. The latter is usually discussed as the consequence of a change in the geometry of the BCD chromophore.[22–23] Because tetracyclines degrade rapidly at pH > 11, most determinations of pK_a values were performed for pH < 11. To the best of our knowledge, only one attempt was made to establish the pK_a of OH10 in aqueous solution.[24] Potentiometric measurements gave an estimate of $pK_{a4} \approx 11.75$, and spectrophotometric experiments yielded $pK_{a4} \approx 11.81$. Quantum chemical calculations by the same authors suggested $pK_{a4} \approx 13$.

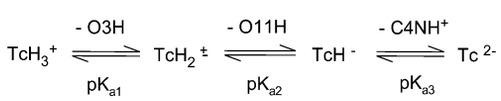

Scheme 2 Abbreviations used for the description of the different protonation/deprotonation equilibria.

The changes in the state of protonation (and conformation) with increasing pH also cause pronounced changes in the appearance of the steady-state fluorescence spectra [Fig. 1(B), $\lambda_{ex} \approx 360$ nm]. Since the emission originates from the BCD chromophore, the differences are most pronounced upon

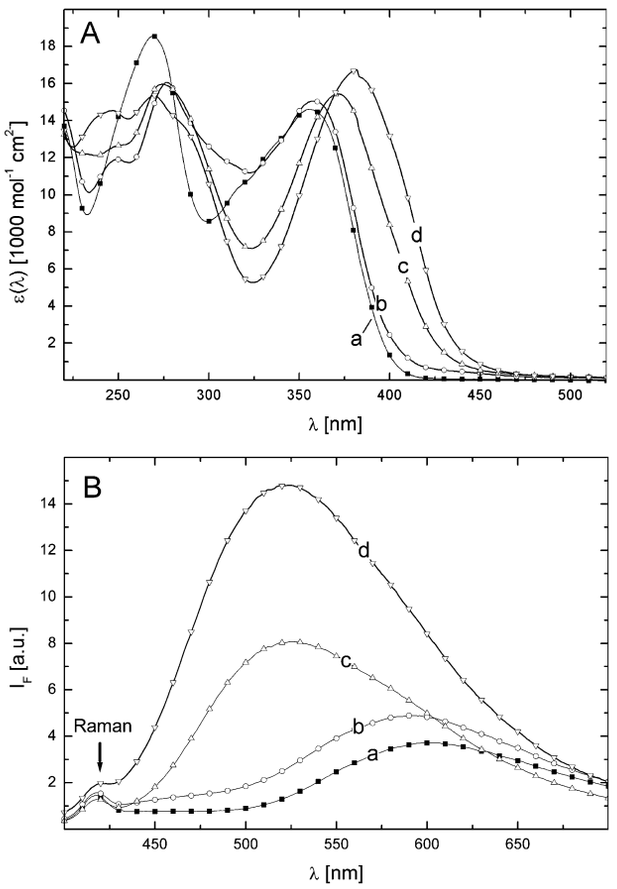

Fig. 1 Absorption (A) and fluorescence (B) spectra (λ_{ex} = 365 nm) of tetracycline in H_2O for different states of protonation as obtained by a principal component analysis of the set of spectra recorded in titration experiments:[21] (a) fully protonated form, tcH_3^+; (b) zwitterionic form, $tcH_2^\pm$; (c) monoanion, tcH^-; (d) dianion, tc^{2-}.

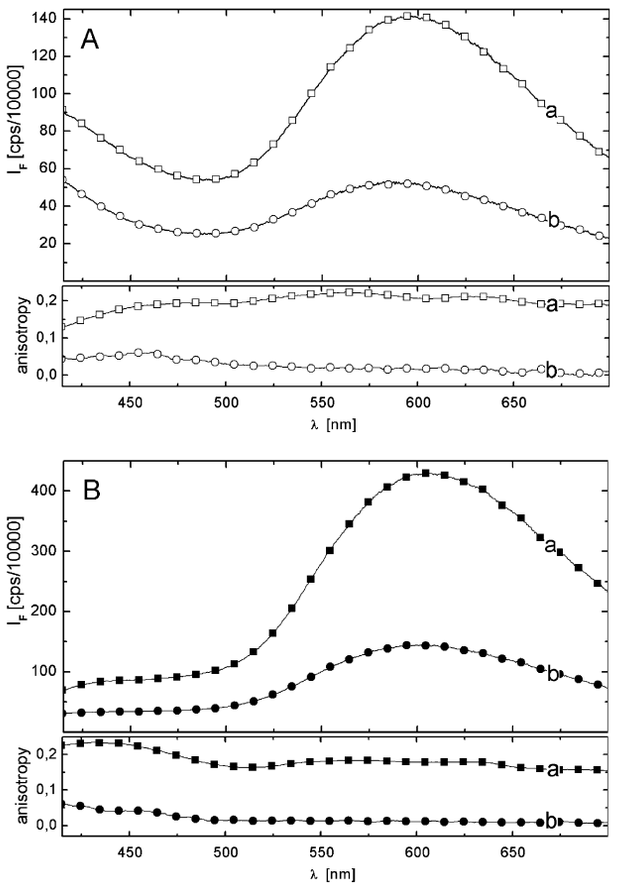

Fig. 2 Steady-state fluorescence spectra of tetracycline and associated anisotropy in acidified H_2O (A) and D_2O (B) recorded at 295 K. Excitation wavelengths, λ_{ex}: (a) 360; (b) 280 nm.

deprotonation of OH12 and, due to the proposed conformational change, upon deprotonation of N4. The steady-state emission spectrum of the fully protonated form (tcH_3^+) shows a maximum around 600 nm and, in addition, a weaker band in the range 400–500 nm whose relative intensity varies with H/D exchange (Fig. 2). If the main emission maximum at 600 nm is related to the absorption maximum at 360 nm, then the extremely large Stokes shift of approximately 240 nm, or about 11 000 cm^{-1}, is obtained. Such large Stokes shifts are generally observed only if intramolecular proton transfer or deprotonation occurs in the excited state.[26] In the zwitterionic form ($tcH_2^\pm$), the Stokes shift is somewhat reduced because the absorption spectrum is slightly bathochromically shifted and the fluorescence spectrum slightly hypsochromically shifted. A more significant decrease in the Stokes shift is found for the monoanion (tcH^-) and dianion (tc^{2-}).

Further evidence that the total fluorescence of tcH_3^+ is composed of at least two different contributions is provided by the course of the degree of anisotropy (Fig. 2). For $\lambda_{ex} \approx 350$ nm, it is a little higher in the blue than in the red emission band. In addition, a small but significant decrease in the anisotropy is found in the long wavelength tail above about 640 nm (we estimate the uncertainty in the determination of the anisotropy to be about 0.005). For short wavelength excitation, the anisotropy is only slightly above zero, with a tendency to higher values in the blue emission band.

The compound in acidified deuterated solution exhibits qualitatively the same fluorescence behavior as the protonated species, except that the fluorescence intensity is generally higher, and, for short wavelength excitation, the relative intensity of the blue fluorescence band slightly lower. For long wavelength excitation, somewhat lower values are obtained for the fluorescence anisotropy in the deuterated system and the change in fluorescence anisotropy around 650 nm does not show up. In both solvents, the fluorescence yield is reduced by a factor of about 4 when the excitation wavelength is changed from 350 to 280 nm, and the relative intensity of the blue emission band enhanced. This implies that the excited A chromphore experiences other relaxation pathways in addition to internal conversion (energy transfer) to the BCD chromophore.

The fluorescence spectra displayed in Fig. 1(B) demonstrate, *via* a comparison with the Raman signal of the solvent around 420 nm, how weak the fluorescence of tetracyclines is in aqueous solution. They also reflect immediately the relative fluorescence yields of tetracycline in various states of protonation. The lowest yields are found for the fully protonated form, tcH_3^+ ($\phi \approx 2.9 \times 10^{-3}$), and the zwitterionic form, $tcH_2^\pm$ ($\phi \approx 4.3 \times 10^{-3}$). The fluorescence yield increases by a factor of about 2 in the monoanion ($\phi \approx 6.9 \times 10^{-3}$) and by another factor of about 2 when going to the dianion ($\phi \approx 13.7 \times 10^{-3}$). Our fluorescence yields were determined relative to that of Rhodamine 6G in water, with $\phi_F = 0.90$. Morrison *et al.*[25] reported fluorescence yields of tetracycline in aqueous solution ($\lambda_{ex} \approx 355$ nm) of 3.7×10^{-4} (pH 5.5) and 14×10^{-4} (pH 8.5). We cannot explain the apparent discrepancy of roughly a factor of ten. The extremely low fluorescence yield explains why conventional single-photon timing techniques cannot successfully be applied to determine the fluorescence decay kinetics.

In Fig. 3, the fluorescence excitation spectra for tetracycline in acidified H_2O and D_2O recorded at different detection wavelengths (λ_{det}) are shown. For easier comparison, they are normalized at the wavelength of the red absorption maximum at about 360 (D_2O) and 365 nm (H_2O). (Because of the low fluorescence yield, the excitation spectra recorded at detection

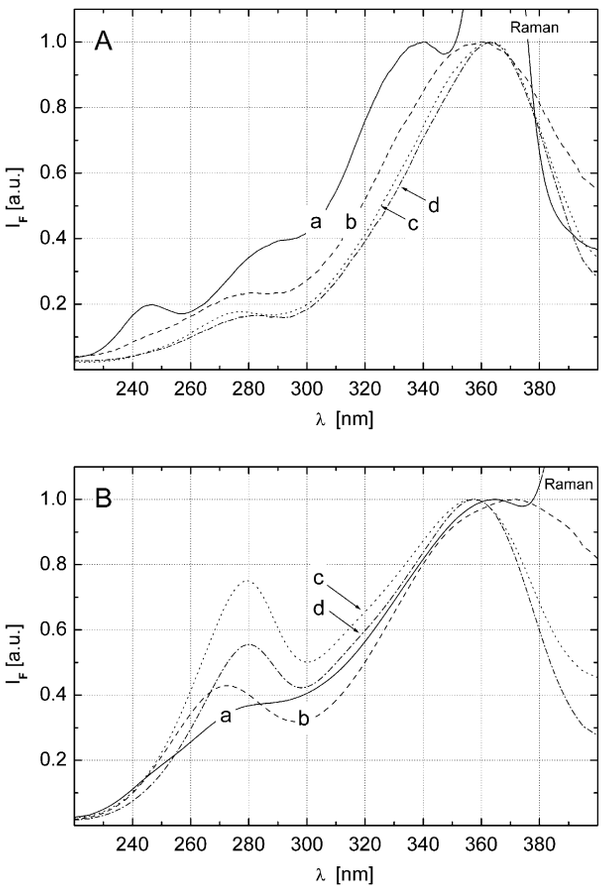

Fig. 3 Normalized fluorescence excitation spectra recorded in acidified H_2O (A) and D_2O (B). Detection wavelengths, λ_{det}: (a) 420; (b) 520; (c) 595; (d) 695 nm.

wavelengths below about 450 nm contain contributions due to Raman scattering. These shift the first maximum towards shorter wavelengths!) Common to both solvents is a variation of the second maximum in the wavelength range 260–290 nm in response to a change in detection wavelength. If the latter is chosen around the fluorescence maximum (~590 nm), then the peak in the excitation spectra appears at somewhat shorter wavelengths than with $\lambda_{det} > 690$ nm or $\lambda_{det} \approx 420$ nm. This hints to a heterogeneity of the absorbing species (*e.g.* tautomers or rotamers). But it could also be a consequence of the fact that tetracycline represents a bichromophoric system (see below).

In the protonated system, an additional peak is seen if the fluorescence is monitored in the blue spectral region. This could again be a clue to the existence of an additional ground-state species. Alternatively, one could imagine a relaxation path, whose efficiency is different in the protonated and deuterated sample.

If the temperature is raised from about 5 to 40 °C, then both the fluorescence intensity and the degree of fluorescence anisotropy decrease continuously. An Arrhenius plot of the fluorescence intensity *versus* $1/T$ (not shown) yields formal activation energies of −6.74 (protonated) and −8.16 kJ mol^{-1} (deuterated sample).

3.2 Time-resolved fluorescence spectra of acidified solutions

Fig. 4 shows for comparison the time-resolved fluorescence spectra of tetracycline dissolved in acidified H_2O and D_2O. For negligible delay time, the relative contribution in the blue spectral region is larger in the deuterated solvent. Furthermore, the decay of the blue part of the emission is extremely fast (Fig. 5). The red part of the fluorescence decays distinctly more slowly, but not according to a mono-exponential decay law. The shorter decay times in the red spectral region are of the order of 25 (H_2O) and 70 ps (D_2O). The longer decay time, which is of the order of 200 ps, cannot be estimated accurately because the dynamic range is too low and the time window too short. However, longer decay times might be influenced by oxygen quenching and, therefore, would be less precise in this experiment.

The described differences in fluorescence-decay kinetics for protonated and deuterated sample can be taken as evidence that intra- and intermolecular hydrogen (deuterium) bonding are essential for the fast radiationless deactivation of electronically excited tetracyclines. Further evidence for this assumption can be seen in the emission spectra of tetracycline in the mixed solvent H_2O–MeOH (2 : 1 by volume). Here, the blue contribution is only about one half of that observed in neat H_2O [Fig. 4(C)].

Within experimental accuracy, the spectral distribution of both emission bands is essentially independent of the type of solvent used. Furthermore, it does not change with increasing delay time after excitation. This observation implies that there is no gradual wavelength shift because of solvent reorganization or (slow) structural relaxation of the solute. This means that whatever process is causing the large Stokes shifts, it must occur on a (sub-)picosecond timescale.

3.3 Time-resolved fluorescence spectra of alkaline solutions without and with divalent metal ions

Time-resolved fluorescence spectra of the tetracycline dianion (tc^{2-}) in alkaline H_2O are shown in Fig. 6(A). In contrast to the spectra of tetracycline in acidified solutions (tcH_3^+), the very broad emission spectrum exhibits only one maximum that, at short delay times, is located at approximately 515 nm. This means that the Stokes shift of tc^{2-} is dramatically reduced *versus* that of tcH_3^+, and amounts to 'only' about 135 nm or approximately 6900 cm^{-1} (*versus* 240 nm of tcH_3^+). The spectral distribution seems to vary with delay time, thereby hinting at the existence of a second emitting species. The fluorescence spectrum observed for delay times longer than about 50 ps peaks around 525 nm and exhibits a long tail towards longer wavelength, in accordance with the steady-state spectrum [Fig. 1(B)]. Since, on the fast timescale, no time-dependent spectral shifts are apparent, it must again be concluded that the process, which causes the still fairly large Stokes shift, is occurring on a (sub-)picosecond timescale.

The shorter decay time of the main fluorescence component ($\lambda_m \approx 515$ nm) is again of the order of several tens of picoseconds (Fig. 7). At the longer detection wavelength, a second decay time of about 160 ps can be detected.

In the wavelength range around 450 nm, the decay is dominated by a low intensity component with a lifetime of only a few picoseconds. In accordance with this finding, a weak shoulder is observed in the steady-state fluorescence spectra [Fig. 1(B)]. UV/vis absorption and fluorescence titration experiments[22] as well as Raman spectra[27,28] proved that at high pH the tetracycline dianion forms 1 : 1 complexes with Mg^{2+} and Ca^{2+}, but with both ions being bound at different locations. The time-resolved fluorescence spectra displayed in Fig. 6(B) and (C) demonstrate that the initial spectral distribution of these two types of complexes is very similar, except that the spectrum of the Ca^{2+} complex is shifted towards longer wavelengths by about 10 nm, as is the absorption spectrum. Again we find that for delay times greater than 100 ps, a fluorescence component with a long red tail is left, in agreement with the steady-state fluorescence spectra of both types of metal ion complexes, which exhibit maxima around 540 nm.[21–23]

As in the previously discussed examples, we find an extremely fast decaying component of low amplitude in the wavelength range $400 \leq \lambda/\text{nm} \leq 500$ (Fig. 7). The main fluorescence of the Mg^{2+} complex with a maximum around 530 nm appears non-monoexponential, the two estimated decay times being about 150 and 500 ps. The first decay time of the Ca^{2+} complex is also

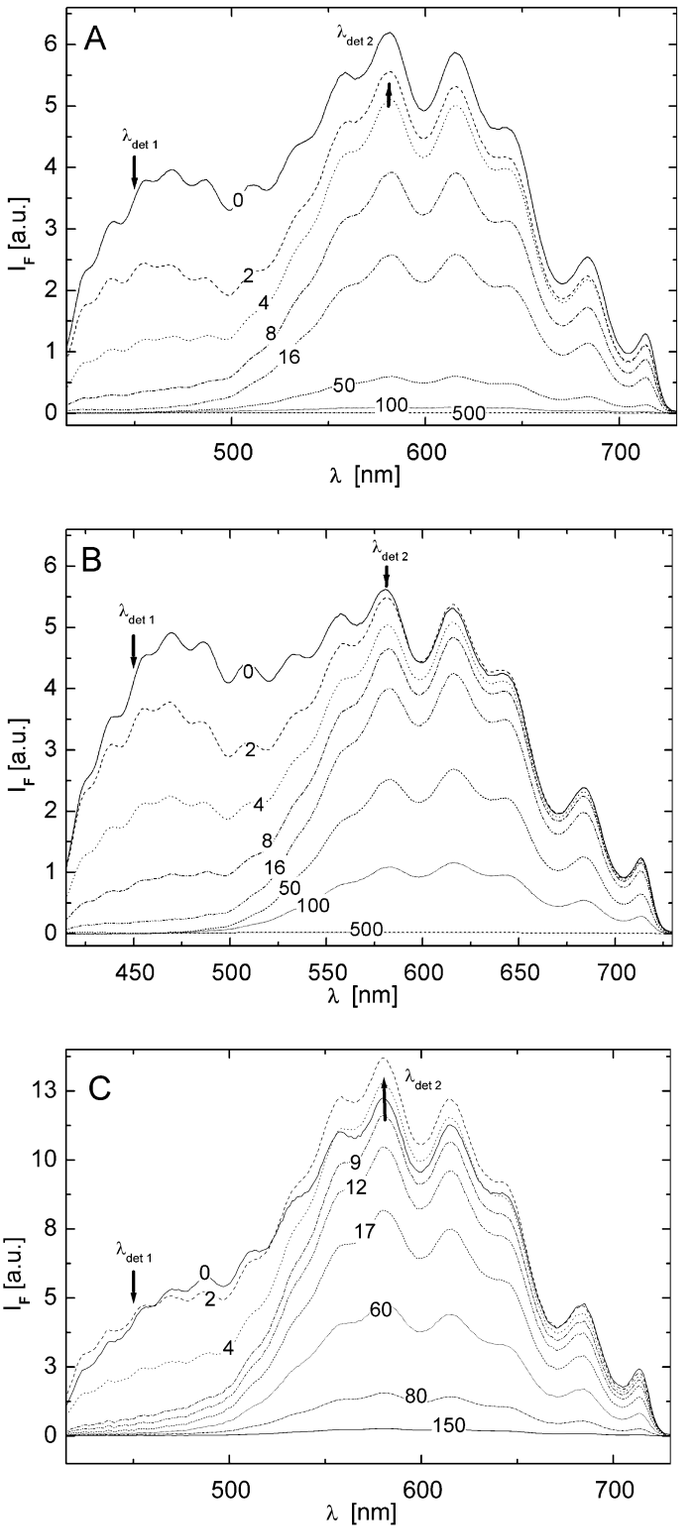

Fig. 4 Time-resolved fluorescence spectra (T = 283 K, λ_{ex} = 266 nm) of tetracycline dissolved in acidified H_2O (A), D_2O (B) and in a H_2O–MeOH mixture (C). Time delays in ps after excitation are indicated on each trace. Fluorescence decay curves for $\lambda_{det\ 1}$ and $\lambda_{det\ 2}$ are shown in Fig. 5.

about 150 ps, but the second is somewhat shorter, namely 320 ps. That the steady-state fluorescence intensity of the Mg^{2+} complex increases if acetonitrile is added to the solution[29] can be taken as further evidence that intermolecular hydrogen bonding is also an important factor in determining the rate of radiationless deactivation of the complexes of tetracycline with divalent metal ions.

3.4 Time-resolved fluorescence spectra at intermediate pH

The pK_a values of tetracycline are: pK_{a1} ≈ 3.3, pK_{a2} = 7.7, pK_{a3} = 9.5.[22,23] Therefore, one can expect that around pH 5.5, the zwitterionic form ($tcH_2^{\pm}$) is the dominant species and that around pH 8.5, the monoanion (tcH^-) predominates. As discussed above, large spectral changes of the absorption band around 360 nm related to the BCD chromophore are seen upon transition from the zwitterion to the monoanion, when the proton at O12 is released [Fig. 1(A)]. The changes in the steady-state fluorescence are in accordance with this observation, as are the changes in the spectral distribution of the fluorescence at short delay times (Fig. 8). There are only small changes between the spectra of $tcH_2^{\pm}$ [Fig. 8(A)] and tcH_3^+. The presence of a

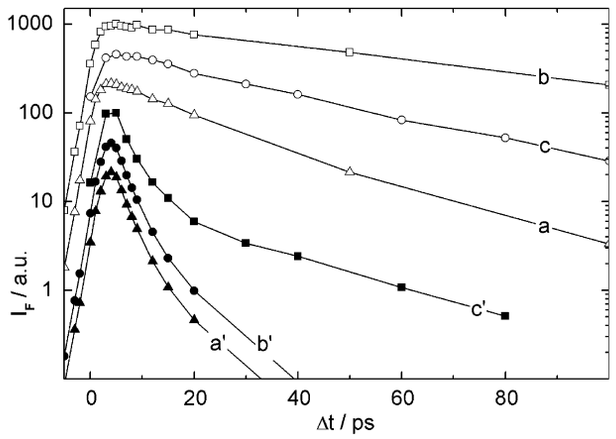

Fig. 5 Fluorescence decay of tetracycline in acidified H_2O (a, a′), D_2O (b, b′) and in a H_2O–MeOH mixture (c, c′). $\lambda_{det\ 1}$ = 580 nm (a, b, c), $\lambda_{det\ 2}$ = 450 nm (a′, b′, c′).

longer-lived component in the decay of the zwitterion is clearly seen in the decay curves recorded around the maximum at about 515 nm (Fig. 9). However a pronounced change occurs upon transition to the monoanion [Fig. 8(B)]. Its initial fluorescence spectrum closely resembles that of tc^{2-} [Fig. 6(A)].

4 Discussion

4.1 Molecular structure in solution

Before a discussion of the deactivation channels of excited tetracyclines can be entered into, the possible molecular structures in solution must be clarified. If tetracycline hydrochloride is crystallized from non-aqueous solution (*e.g.* MeOH), then it exists in the crystal in its fully protonated state, tcH_3^+. The arrangement of the functional groups attached to ring A is shown in Scheme 3(b). Two intramolecular hydrogen bonds at the BCD fragment are formed between O11 and OH10 and OH12 (Scheme 4, structure **A**).[30,31]

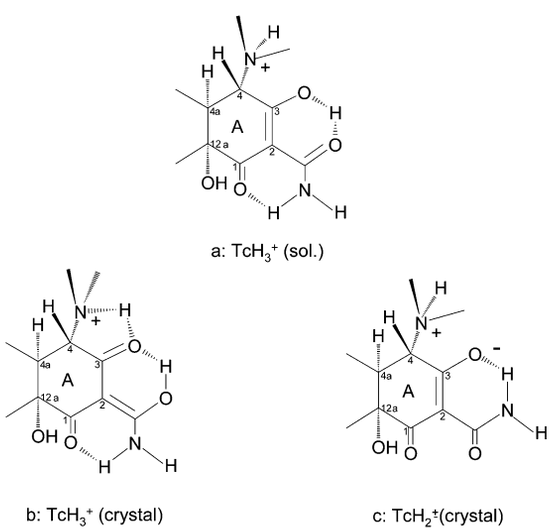

Scheme 3 Arrangement of the functional groups attached to ring A in solution (postulated) (a) and in crystalline (X-ray structure) tetracycline hydrochloride (b) and tetracycline hexahydrate (c).

If tetracycline is crystallized from aqueous solution, it adopts the zwitterionic form independently of the pH of the mother liquor. Different intramolecular hydrogen bonds between the substituents of ring A are formed because the carboxamide group is rotated by 180° [Scheme 3(c)]. The same intramolecular hydrogen bonds are formed on the BCD fragment between O11

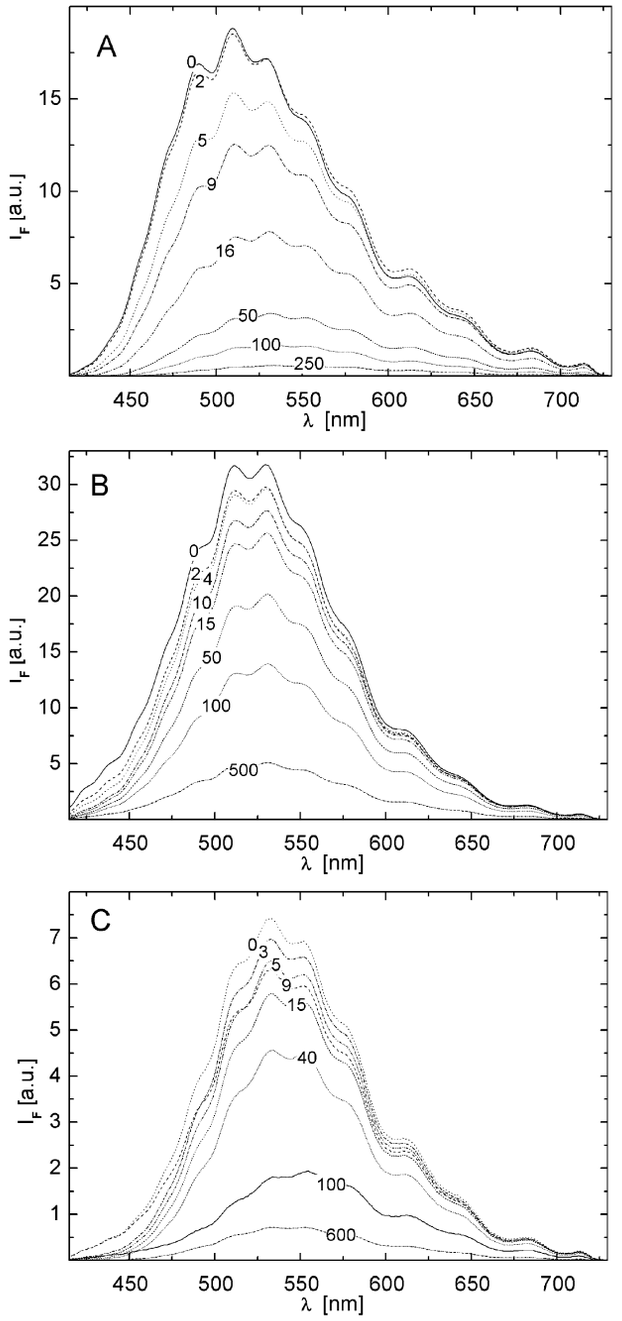

Fig. 6 Time-resolved fluorescence spectra (λ_{ex} = 266 nm) of tetracycline dissolved in alkaline H_2O (A) and with approximately equimolar amounts of Mg^{2+} (B) or Ca^{2+} (C) added. Time delays in ps after excitation are indicated on each trace.

and OH10 and OH12. In the tetracycline hexahydrate crystal, intermolecular hydrogen bonds between water of crystallization and functional groups of tetracycline can be identified. Acceptors of hydrogen bonds are O1, O2 and O12a, whereas N4H, OH6 and OH12a act as donor groups. Inclusion of this hydrogen-bonding network in quantum-chemical calculations is essential for their outcome.

The difference in crystal structure between $tcH_2^{\pm}$ (zwitterion) and $tcH_3^+Cl^-$ manifests itself clearly in the IR- and NIR-FT Raman spectra of the crystalline material. A comparison of the experimentally observed bands with the results of quantum chemical calculations (BP86) suggests that, in accordance with the similarity in structure, the bands related to the BCD chromophore are largely unchanged for both species.[28] For normal modes located on the A ring, the calculations predict significant differences. Therefore, the majority of the non-conserved bands should be related to the A ring and its

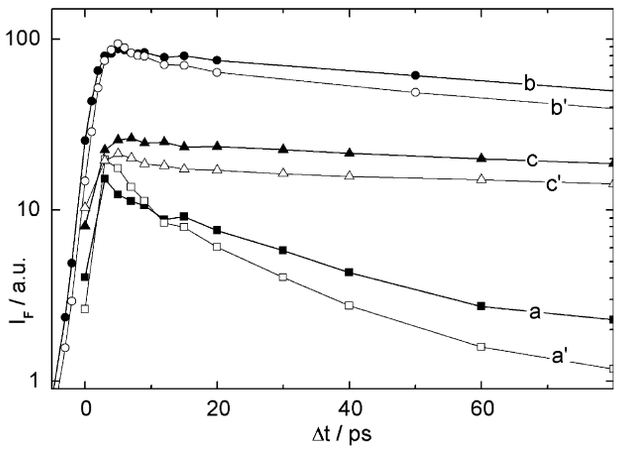

Fig. 7 Comparison of the fluorescence decay of tetracycline dissolved in alkaline H_2O (a, a′) and its complexes with Mg^{2+} (b, b′) and Ca^{2+} (c, c′). $\lambda_{ex} = 266$ nm; $\lambda_{det} = 480$ (a, b, c), 580 nm (a′, b′, c′).

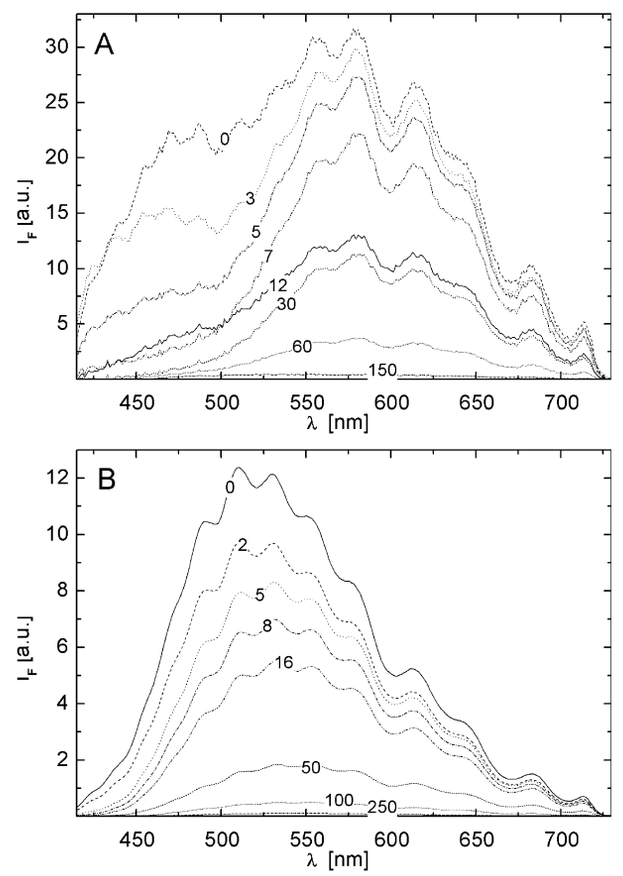

Fig. 8 Time-resolved fluorescence spectra (λ_{ex} = 266 nm) of tetracycline dissolved in H_2O at intermediate pH: (A) pH 5.2; (B) pH 8.5.

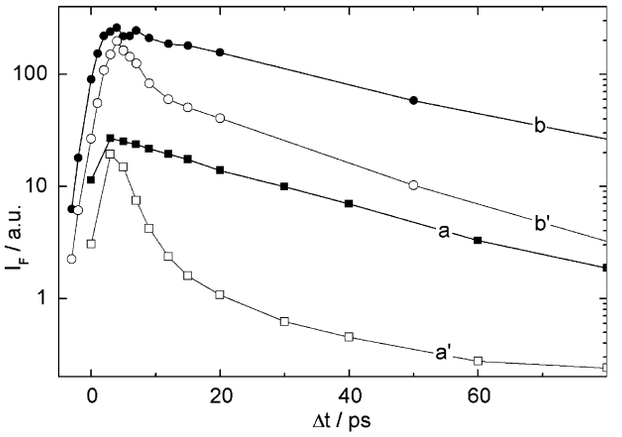

Fig. 9 pH dependence of the fluorescence decay of tetracycline in H_2O monitored around the fluorescence maxima: (a) pH 5.2 (λ_{det} = 590 nm); (a′) pH 5.2 (λ_{det} = 450 nm); (b) pH 8.5 (λ_{det} = 515 nm); (b′) pH 8.5 (λ_{det} = 450 nm).

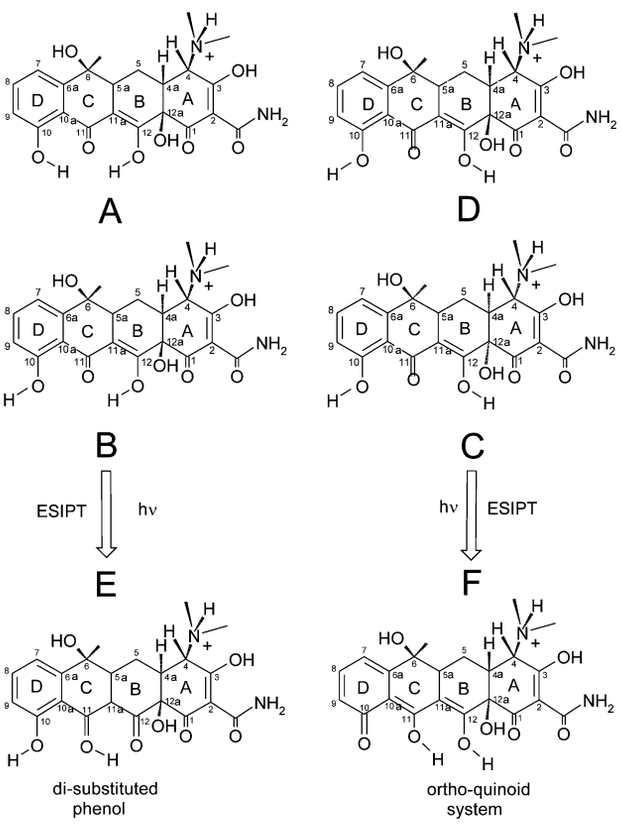

Scheme 4 Tautomers of tetracycline for which DFT calculations have been performed. Excited-state proton transfer would lead to isomers **E** and **F**, which are unstable in the electronic ground state.

substituents. Since the NIR Raman spectra of crystalline $tcH_3^+Cl^-$ and of the acidified solution of tc show pronounced differences for those bands which are most likely related to the A ring and its substituents, it must be concluded that in aqueous solution, a mixture of the isomers shown in Scheme 3 is present.

It is generally assumed that the electronic properties of the BCD chromophore (excitation energies, oscillator strengths) are barely influenced by a change in the tautomeric/rotameric distribution of the substituents of ring A. It has, however, been suggested, without real proof, that a change in the intramolecular hydrogen-bonding pattern of the substituents of ring A could induce a significant change in the molecule skeleton, mainly the orientation of ring A *versus* the plane spanned by rings B, C and D. Another consequence of this could be a change in the intramolecular hydrogen-bonding pattern around OH10, O11 and OH12, including even intermolecular hydrogen bonding to solvent molecules.

Taking together all of the presented facts, we must consider the possibility that, in solution, not only the UV/vis absorption bands originating from the A chromophore, but also the long wavelength absorption band due to the BCD chromophore are inhomogenously broadened due to different intra- and intermolecular hydrogen-bonding patterns. Further experimental evidence for this conclusion is provided by the results of hole burning experiments (unpublished results of Prof. J. Friedrich, TU München, Germany).

The consideration of various tautomeric/rotameric equilibria connected with the isomers displayed in Scheme 3 for the fully protonated species also has a consequence with respect to the

deuterium isotope effect. Taking into account only isomer **A**, then, besides O12H, only N4H and O3H should be subject to H/D exchange in solution.

4.2 Steady-state spectra

It has been pointed out in a previous section that the total fluorescence yield of tetracyclines in aqueous solutions is extremely low, thereby indicating the existence of very effective channels for non-radiative decay. The spectral distribution of the steady-state emission spectra and the recorded anisotropy (λ_{ex} = 350 nm) provide, in combination with the fluorescence excitation spectra, evidence that there are at least three different emitting states involved. This is confirmed by the analysis of the fluorescence decay curves.

The emission in the short wavelength range below about 500 nm is very weak, but since its decay time is also extremely short, its radiative rate ($k_r = \Phi/\tau$) could be still in the 'normal' range. The main contribution at short delay times peaks around 600 nm, its spectral distribution appears to be essentially independent of H/D exchange. The latter has, however, a significant effect on the decay time of the longer-lived component. For delay times of 100 ps or more, almost no fluorescence remains in H_3O^+, whereas in D_3O^+, a weak but non-negligible contribution is left, with its spectral distribution being bathochromically shifted. This can eventually explain why the steady-state spectra exhibit a long tail in the red and why the maximum in D_3O^+ appears bathochromically shifted by about 15 nm *versus* the spectrum in H_3O^+. The time resolution of our experiment is not appropriate to determine the deuterium isotope effect on the fluorescence lifetimes of the very short- or long-lived components. For the intermediate one, the increase in the lifetime in the deuterated system can be clearly seen (Fig. 5).

The above-mentioned decrease in the fluorescence anisotropy with increasing temperature could, in principle, be related to faster orientational relaxation due to lower solvent viscosity. But comparison of the absolute values of the fluorescence anisotropy observed in H_3O^+ and D_3O^+ with λ_{ex} = 350 nm provides evidence against this hypothesis. Since the decay time of the predominant component with intermediate lifetime is larger in D_3O^+ than in H_3O^+, one would expect a lower anisotropy in the latter solvent, provided all other parameters are the same.

In case of short wavelength excitation, it is most likely that the absorption dipole has a different direction than the emitting dipole located on the BCD chromophore, independent of whether the primary absorbing species is the A or BCD chromophore. Consequently, the anisotropy should show a lower value than with excitation at 350 nm. Note that the 'blue' part of the fluorescence exhibits again a somewhat higher anisotropy than the main component and, in contrast to excitation around 350 nm, no change in anisotropy is observed around 650 nm. Both observations can be reconciled by the assumption that the transition dipole moments to higher excited states are at different angles to the transition dipole moment of the 'blue'- and 'red'-emitting state.

The intensity decay of the dominant component with intermediate lifetime exhibits, in the temperature range investigated, an Arrhenius-type behavior. If we assume the radiative transition rate, k_r, to be less sensitive to temperature, then we can relate the decrease in intensity, I, to a decrease in lifetime or an increase in the rate of radiationless transition, $k_{nr} = k_{nr}' + k_{nr}''(T)$:

$$\frac{I(T_1)}{I(T_2)} = \frac{\Phi(T_1)}{\Phi(T_2)} = \frac{k_r \Big/ \left[k_o + k_{nr}''(T_1)\right]}{k_r \Big/ \left[k_o + k_{nr}''(T_2)\right]} = \frac{k_o + k_{nr}''(T_2)}{k_o + k_{nr}''(T_1)}$$

where $k_o = k_r + k_{nr}'$ represents the sum of radiative and temperature-independent radiationless deactivation.

At the high temperature limit [$k_o \ll k_{nr}''(T)$], the formal activation energy derived from the Arrhenius plot of the fluorescence intensity, E_A^F, would directly correspond to the (positive) value of the activation energy, E_A^R, of the temperature-induced radiationless deactivation process $k_{nr}''(T) = k_{nr}^o \exp(-E_A^R/RT)$. At the low temperature limit [$k_o \gg k_{nr}''(T)$], the true activation energy for the radiationless process, E_A^R, appears with a negative scaling factor in the Arrhenius plot of the intensity:

$$E_A^F \approx -(k_{nr}^o/k_o)E_A^R$$

Because the apparent activation energy E_A^F is negative, the high temperature limit should be the appropriate treatment. This means that the activation energy of the temperature-dependent radiationless process must certainly be smaller than the absolute values derived from the Arrhenius plot of the fluorescence intensities [6.74 (H_3O^+) and 8.16 kJ mol^{-1} (D_2O^+)]. Since we have no information about k_{nr}^o/k_o, we cannot make an estimate of the deuterium isotope effect on the activation energy of the temperature-induced radiationless process. But activation energies below 8 kJ mol^{-1} should not rule out intramolecular proton transfer.

4.3 Time-resolved experiments

The time-resolved experiments are unable to detect a difference in the kinetics of the fluorescence rise for excitation pulses at 386 or 266 nm. This could indicate that the lifetime of the excited A chromophore is extremely short or that the yield of energy transfer to the BCD chromophore is low, in accordance with the results of the steady-state fluorescence measurements. Regarding the many possibilities for intramolecular hydrogen bonding within the substituents of the A chromophore, high rates for non-radiative deactivation cannot be a surprise. If the yield of energy transfer is low, then the fluorescence monitored in the time-resolved experiments with 266 nm excitation would originate preferentially from those molecules in which photon absorption leads to excitation into a higher excited state of the BCD chromophore followed by rapid internal conversion. Under this assumption, the reduction of fluorescence upon short wavelength excitation reflects the ratio of the absorption coefficients of the A and BCD chromophores around 266 nm.

In a study of the photochemical and photophysical properties of tetracyclines, Morrison *et al.*[25] suggested that the de-(dimethylamino)tetracycline (DTc) and lumitetracycline (LTc) are formed *via* two different triplet states of tetracycline. That which yields DTc is populated only after excitation at very short wavelengths and does, in their model, not convert readily into the lower energetic triplet state. As proven by sensitizing experiments, the latter yields LTc. One can therefore speculate that the excited A chromophore decays preferentially into the triplet-state manifold of the A chromophore. Furthermore, interconversion of the triplet state of the A chromophore to the triplet-state manifold of the BCD chromophore should possess only a low probability. Recently performed picosecond time-resolved transient absorption measurements show that the spectral distribution of the optical density change, which persists beyond a 2 ns delay time, is different for excitation at 400 and 266 nm. Since, at this delay time, the fluorescing states have decayed, this weak, longer-lived transient absorbance could be due to triplet states, as suggested by Morrison *et al.*, but also to (meta)stable photoproducts formed *via* fast singlet reactions.

To make a guess on the non-radiative deactivation process(es) of the BCD chromophore is more difficult. It is intriguing to assume that breaking of intramolecular hydrogen bonds and/or proton transfer (Scheme 4) of OH10 or OH12 are good candidates.[25,29] Therefore, it is worth discussing the behavior of the dianion in comparison with its complexes with divalent metal ions.

Upon complexation of the tetracycline dianion with Mg^{2+} or Ca^{2+}, large changes in the UV/vis absorption spectra are observed below 350 nm.[21–23] But the red absorption band (370 nm) also shifts bathochromically by about 10 (Mg^{2+}) or 12 nm (Ca^{2+}). In addition, a shoulder shows up around 390 (Mg^{2+}) or 400 nm (Ca^{2+}), thereby making the long wavelength tail much steeper than in the spectrum of the metal-free dianion (tc^{2-}). Although it has been suggested that metal ion complexation should involve the functional groups on ring A, we take our Raman spectra as evidence that, at least in the majority of tetracyclines, the complexation site involves O11 and O12 (Mg^{2+}) or O12 and O1 (Ca^{2+}).[28] In view of the possible isomeric structures of the ring A substituents (Scheme 3), it could be speculated that, as a consequence of metal ion complexation, the distribution of isomers is changed in favor of one form. In any case, OH12 is released and, consequently, the possibility of forming an intramolecular O12H–O11 hydrogen bond eliminated. But O10H can still be engaged in intra- or intermolecular hydrogen bonding.

The lack of a strong fluorescence component with $\lambda_m \approx 600$ nm in the time-resolved emission spectra of the three samples investigated (tc^{2-} and the corresponding complexes with Mg^{2+} or Ca^{2+}) provides strong evidence that (intramolecular) proton transfer involving OH12 is a major route for radiationless deactivation of the fully protonated system and that the emission with a maximum around 600 nm must be assigned to fluorescence from a proton-transferred form; its transition dipole moment could naturally be oriented under a certain angle relative to that of the absorbing isomer, thus explaining the lower degree of anisotropy.

Since only the steady-state fluorescence spectra are corrected for the spectral sensitivity of the detection system, and because of the undulations in the time-resolved spectra, it is impossible to check whether the emission maximum observed in the time-resolved spectra of the metal ion complexes matches perfectly that of the steady-state spectra. Since the latter appears a little bit bathochromically shifted, it could be a hint for a longer-lived component with a rather broad spectral distribution.

The actual presence of such a longer-lived component with a significant tail extending into the red spectral region is clearly observed in Fig. 5(B) and (C). Assuming that the site of metal ion complexation stays unchanged during the excited-state lifetime, then the red-emitting species must exhibit an internal degree of freedom, which can give rise to long progressions, *e.g.* torsion around a single bond or weak hydrogen bonding. Alternatively, it could be proposed that the second contribution originates from complexes with a different binding pattern in the ground state. Since we do not have the necessary information (equilibrium concentrations, absorption coefficients at the excitation wavelength, fluorescence yields) it is impossible to distinguish between these alternatives. In any case, this long-lived fluorescence component should be related to an emissive state which is not formed *via* proton transfer involving OH12. This finding can help to rationalize why the Stokes shift is greatly reduced compared to those of tcH_3^+ and $tcH_2^{\pm}$ (see below).

The increase in the lifetime of the strong component with intermediate lifetime by about a factor of 5 upon complexation with Mg^{2+} is in accord with the increase in overall fluorescence yield. The lifetime of the intermediate component of metal-free tc^{2-} is, however, not much changed *versus* that found for tcH_3^+. Therefore, the observed increase in steady-state fluorescence yield must, at least in part, be due to a reduction of that species which exhibits the ultra-short lifetime in the protonated state.

Further support for the above-outlined hypotheses can be found in the time-resolved fluorescence spectra at intermediate pH, where the zwitterion (pH 5.2) and the monoanion (pH 8.5) should prevail.[21–23] At pH 8.5, the spectral distribution monitored for small delay times resembles closely that found at pH 11 [Fig. 8(A)]. The steady-state fluorescence yield of the monoanion is, however, lower by a factor of two than that for pH 11. The reason is probably that the major component found at pH 11 splits up into two fractions, one of which shows about the same decay time. But there is a second component with a significantly reduced decay time and, most likely, with a reduced fluorescence yield [Fig. 9(b) and (b′)]. As at pH 11, there is a fairly long-lived component which extends far into the red spectral region.

The initial spectral distribution found at pH 5.2 closely resembles that found for tcH_3^+ at pH 2. The main component again peaks around 590 nm, suggesting that it could be an emission from a state which is formed by ultra-fast intramolecular proton transfer of OH12. Its decay time is also similar, indicating that deprotonation of the substituents of ring A has only a minor effect on the decay time of the BCD chromophore. Below 500 nm, a fast decaying component is again found, but with a slightly higher relative intensity. Here again, it can be concluded that the existence and decay kinetics of this component must be independent of the state of protonation of the A chromophore.

4.4 Excited-state intramolecular proton transfer

Past investigations dealing with the ground-state properties of tetracyclines uniformly assumed that the pK_a of OH10 is above 11. This means that this phenolic group is essentially conserved in the ground state under all experimental conditions employed in this study. Morrison *et al.*[25] speculated that in the excited state, the acidity of O10 is increased and that of O11 decreased to such an extent that proton transfer will actually occur as a primary photophysical step in competition with deprotonation of O10. These authors also discussed a double proton transfer step involving the keto group at C1. The latter process could be influenced by the tautomeric structure of the A chromophore. Formally, OH10–O11 proton transfer in the fully protonated form tcH_3^+ or in the zwitterion $tcH_2^{\pm}$ leads to a π-electron system with *ortho*-quinoid structure [Scheme 4(F)]. In contrast, the product of OH12–O11 proton transfer [Scheme 4(E)] can be classified, like the educt species **A**, as a disubstituted phenol.

To get an estimate on the spectral shifts connected with the structural changes outlined in Scheme 4, we have performed DFT calculations for the zwitterionic form ($tcH_2^{\pm}$). This form was chosen for computational reasons. It has been pointed out before that deprotonation of N4 should have only a minor effect on the energetics of the BCD chromophore. In accord with the X-ray structure, the isomer **A** is predicted to be the most stable one (Table 1). The reason for the high stability is found in the two very strong intramolecular hydrogen bonds, OH10–O11 and O11–OH12 (Table 2). All other isomers, which lack at least one of these hydrogen bonds, are significantly higher in energy. Although incorporation of intermolecular hydrogen bonding to solvent molecules could change the energetic ordering of the other isomers, isomer **A** should remain the most stable.

Breaking of either one of the two intramolecular hydrogen bonds of isomer **A** (Scheme 4) results in a significant increase in the calculated energy difference between the ground and lowest excited electronic state (Table 1). Since, according to the calculations, the lowest singlet state of isomers **A** and **B** has strong CT character, its energy should be influenced by the extent of solvation (hydrogen bonding) of the A ring and its substituents. The calculations, which include six water molecules, predict the lowest excited state of these two isomers to represent a typical π(BCD) ⟶ π*(BCD) transition at about 355 nm, which is in fair agreement with experiment (Table 3).

The optimization procedure for the geometry of the first excited state of isomers **A** and **C** does not produce a relaxed geometry which could be interpreted as the result of an intramolecular proton transfer process. But for isomer **B**, which exhibits only the intramolecular hydrogen bond from OH12 to

Table 1 Results of DFT calculations (TDDFT/B3LYP, TZVP) for tetracycline zwitterions (isolated molecule). $\Delta E°(0\ K)$ (in eV/kJ mol^{-1}) represents the electronic energy at 0 K without zero-point energy correction relative to the most stable isomer, **A**, and ΔE the vertical excitation energy (in eV/nm). Because there is no strict σ–π separation, the classification given (footnotes *a–d*) is only an illustration. The structures of the isomers **A**–**F** are shown in Scheme 4

Isomer	A	B	C	D	E	F
$\Delta E°(0\ K)$	0.0/0.0	0.54/52.3	0.53/51.5	1.21/117.0	0.49/46.8	1.57/150.7
$\Delta E(S_0–S_1)$	3.01/411[a]	3.21/386[a]	3.57/347[b]	3.16/393[b]	2.89/429[c]	2.44/508[b]
$\Delta E(S_0–S_2)$	3.11/399[a]	3.32/374[a]	3.60/344[b]	3.87/321	3.03/409[a]	2.88/430[b]
$\Delta E(S_0–S_3)$	3.50/353[a]	3.66/339[b]	3.86/322[a]	4.06/305[b]	3.55/349[a]	3.34/366[d]

[a] CT transition π(A) ⟶ π*(BCD). [b] LE transition π(BCD) ⟶ π*(BCD). [c] n ⟶ π* transition n(O10) ⟶ π*(BCD). [d] CT transition π(BCD) ⟶ π*(A).

Table 2 Intramolecular hydrogen-bonding energies, *E*(hb), in tetracycline zwitterions (isolated molecule), obtained by employing the SEN approach[19] for the TDDFT/B3LYP data (all energies are given in kJ mol^{-1}). The structures of the isomers **A**–**F** are shown in Scheme 4

Isomer	A	B	C	D	E	F
OH10–O11	−46.2		−60.0			
OH12–O11	−62.7	−79.5				
OH12–O12a			−17.9	−18.3		−18.9
OH12a–O12	−5.4	−6.4			−13.6	
OH11–O12					−69.1	−32.0
E(hb)	−114.3	−85.9	−77.9	−18.3	−82.7	−38.9
Relative *E*(hb)	0.0	+28.4	+36.4	+96.0	+31.6	+75.4

Table 3 Results of DFT calculations (TDDFT/B3LYP, TZVP) for tetracycline zwitterions, including six water molecules. ΔE represents the excitation energy (in eV/nm). Because there is no strict σ–π separation, the classification given (footnotes *a–d*) is only an illustration. The structures of the isomers **A**–**F** are shown in Scheme 4. The location of the water molecules was determined by energy optimization

Isomer	A	B	E	F
$\Delta E(S_0–S_1)$	3.50/355[a]	3.61/343	3.47/358[b]	2.43/509[a]
$\Delta E(S_0–S_2)$	3.64/331[b]	3.70/335[b]	3.54/350[a]	2.84/436[a]
$\Delta E(S_0–S_3)$	3.76/330[a]	3.79/327[a]	3.68/337[a]	3.09/401[c]

[a] LE transition π(BCD) ⟶ π*(BCD). [b] CT transition π(A) ⟶ π*(BCD). [c] CT transition π(BCD) ⟶ π*(A).

O11, this is the case, whether water molecules are included in the calculation or not. The lowest electronic excitation energy of the proton-transferred species **E** (Scheme 4) should be reduced by about 0.3 eV *versus* that of the precursor, isomer **B**. Since the lowest energy transition of **F** represents a π(BCD) ⟶ π*(BCD) transition, its energy is not much influenced by the interaction with the surrounding water molecules. In contrast, the lowest excited states of photoproduct **E** exhibit a significant charge-transfer character. Therefore, the calculated excitation energy depends sensitively on solvation.

Adding up $\Delta E°(0\ K)$ and $\Delta E(S_0–S_1)$ for isomers **B** and **E** in Table 1 gives 3.75 and 3.38 eV, respectively. This estimate shows that **E*** is indeed lower in energy than **B***. That energy optimization of **B*** leads to **E*** is indicative of a relaxation pathway without a (high) barrier. Applying the same procedure to isomers **C** and **F**, one gets 4.10 and 4.01 eV as relative energies for **C*** and for **F***, respectively. This could mean that **C*** and **F*** have approximately the same energy and that the excited-state intramolecular proton transfer (ESIPT) process is not observed because of the existence of a (small) barrier in the model calculations for $T = 0$ K. If the latter could be crossed at elevated temperature, then one could rationalize the temperature dependence of the steady-state fluorescence intensity. Because the formation of the isomer **F*** could explain a fluorescence with an extremely large Stokes shift, we tentatively assign the third, long wavelength component to emission from **F***. Its yield of formation and its fluorescence yield can exhibit a large deuterium isotope effect. In solution, the entropic contribution to the Gibbs free energy certainly will be an important factor whether or not ESIPT occurs.

Intermolecular hydrogen bonding most likely can change the predominant decay channels in tetracyclines by changing the sequence of the excited electronic states with different character (LE, CT, n ⟶ π*, etc.). Morimoto *et al.*[32] showed that the primary photophysical processes occurring in 2-piperidinoanthraquinone vary dramatically depending on the orientation of the hydrogen bond formed between the keto group of the excited solute and an OH group of the solvent. If the solvent attack is out-of-plane, a non-emissive complex is formed; but if the attack is in plane, then an emissive complex is produced. The authors suggest that "a bending motion of the carbonyl would effectively couple with the out-of-plane type intermolecular hydrogen bond resulting in a large energy dissipation. The bending mode in this case could be called a promoting mode with the hydrogen bond being an accepting mode in the radiationless transition."

It could be hypothesized that the discussed mechanism could also be effective in tetracyclines, involving the keto group oxygen O11 (BCD chromophore) and O1 (A chromophore). Intramolecular hydrogen bonding to O11 will modify certainly the in-plane attack of solvent molecules, but most likely also the out-of-plane attack. Therefore, the importance of intermolecular hydrogen bonding on the rate of radiationless deactivation could vary strongly between the various isomers. The described mechanism could be helpful to rationalize that the molecules formed by ESIPT, which also contain keto groups, exhibit short lifetimes and low fluorescence quantum yields.

5 Summary and conclusion

The time-resolved fluorescence spectra provide unique evidence that in tetracyclines, several very fast relaxation processes are operative, which lead to several distinct primary photoproducts, thereby causing the apparently large fluorescence Stokes shift in the steady-state spectra. The experimental findings do not allow a distinction between two cases: (i) one predominant isomer is excited and several different relaxation mechanisms (*e.g.* proton transfer, electron transfer, *etc.*) occur in parallel or (ii) several isomers (conformers) coexist in the electronic ground state, each undergoing a structure-specific relaxation process in the excited state.

The DFT calculations for the isolated molecule suggest that ESIPT should occur whenever the keto group oxygen is subject to only one intramolecular hydrogen bond. Proton transfer

from O10 to O11, which yields an *ortho*-quinoid structure (**F***), could easily explain the very large Stokes shift observed for the third fluorescence component. Since it is not predicted as a relaxation process by the geometry optimization procedure of the lowest excited state, a thermally activated process must be considered. ESIPT from O12 to O11 yields a product (**E***), whose fluorescence is expected at somewhat higher energy. Consequently, the dominant fluorescence around 590 nm could represent emission from **E***.

The model calculations also demonstrate that intermolecular hydrogen bonding can dramatically change the ordering of the excited states. Therefore, we are presently performing more calculations to get a better understanding of the solvent effects on the steady-state absorption spectra (inhomogeneous broadening), the spectral distribution of the emission spectra and the photophysical behavior of tetracyclines. Attention will also be focused on the energetics of deprotonation in the excited states of the various isomers.

Time-resolved fluorescence studies provide information on the decay time of the emitting states, but none about the non-radiative decay routes. To close this gap in information, we recently performed transient absorption measurements. They should help to clarify, for example, the importance of inter-system crossing as a deactivation process.

Acknowledgements

The authors thank Dr W. Hillen and Dr T. Clark (Universität Erlangen-Nürnberg, Germany) for many stimulating discussions. Financial support by Deutsche Forschungsgemeinschaft (SFB 473) and Fonds der Chemischen Industrie is gratefully acknowledged. We also appreciate a grant by the European Union TMR Large Scale Facility Access Programme.

References

1 B. M. Duggar, Aureomycin: a product of the continuing research for new antibiotics, *Ann. N. Y. Acad. Sci.*, 1948, **51**, 177–181.
2 *Tetracyclines in Biology, Chemistry and Medicine*, ed. M. Nelson, W. Hillen and R. A. Greenwald, Birkhäuser Verlag, Basel, 2001.
3 R. Hanemaaijer, N. van Lent, T. Sorsa, T. Salo, Y. T. Konttinen, J. Lindeman, Inhibition of matrix metalloproteinases (MMPs) by tetracyclines, in *Tetracyclines in Biology, Chemistry and Medicine*, ed. M. Nelson, W. Hillen and R. A. Greenwald, Birkhäuser Verlag, Basel, 2001, pp. 267–281.
4 W. Hinrichs, C. Kisker, M. Düvel, A. Müller, K. Tovar, W. Hillen and W. Saenger, Structure of the Tet repressor-tetracycline complex and regulation of antibiotic resistance, *Science*, 1994, **264**, 418–420.
5 W. Hinrichs and Ch. Fenske, Gene regulation by the tetracycline-inducible Tet repressor-operator system – molecular mechanisms at atomic resolution, in *Tetracyclines in Biology, Chemistry and Medicine*, ed. M. Nelson, W. Hillen and R. A. Greenwald, Birkhäuser Verlag, Basel, 2001, pp. 107–123.
6 C. Gatz and P. H. Quail, Tn10-encoded tet repressor can regulate an operator-containing plant promoter, *Proc. Natl. Acad. Sci.*, 1988, **85**(5), 1394–1397.
7 M. Gossen and H. Bujard, Tetracyclines in the control of gene expression in eukaryotes, in *Tetracyclines in Biology, Chemistry and Medicine*, ed. M. Nelson, W. Hillen and R. A. Greenwald, Birkhäuser Verlag, Basel, 2001, pp. 139–157.
8 M. Takahashi, J. Degenkolb and W. Hillen, Determination of the equilibrium association constant between Tet repressor and tetracycline at limiting Mg^{++} concentrations: A generally applicable method for effector dependent high affinity complexes, *Anal. Biochem.*, 1991, **199**, 197–202.
9 P. Matousek, M. Towrie, A. Stanley and A. W. Parker, Efficient rejection of fluorescence from Raman spectra using picosecond Kerr gating, *Appl. Spectrosc.*, 1999, **53**, 1485–1489.
10 P. Matousek, M. Towrie, C. Ma, W. M. Kwok, D. Phillips and A. W. Parker, Fluorescence suppression in resonance Raman spectroscopy using a high-performance picosecond Kerr gate, *J. Raman Spectrosc.*, 2001, **32**, 983–988.
11 R. Ahlrichs, M. Bär, M. Häser, H. Horn and C. Kölmel, Electronic structure calculations on workstation computers: The program system turbomole, *Chem. Phys. Lett.*, 1989, **162**, 165–169.
12 A. D. Becke, Density-functional thermochemistry. III. The role of exact exchange, *J. Chem. Phys.*, 1993, **98**, 5648–5652.
13 P. J. Stephens, F. J. Devlin, C. F. Chabalowski and M. J. Frisch, Ab initio calculation of vibrational absorption and circular dichroism spectra using density functional force fields, *J. Phys. Chem.*, 1994, **98**, 11 623.
14 R. Bauernschmitt and R. Ahlrichs, Treatment of electronic excitations within the adiabatic approximation of time dependent density-functional theory, *Chem. Phys. Lett.*, 1996, **256**, 454–464.
15 R. Bauernschmitt, M. Haeser, O. Treutler and R. Ahlrichs, Calculation of excitation energies within time-dependent density functional theory using auxiliary basis set expansions, *Chem. Phys. Lett.*, 1997, **264**, 573–578.
16 R. Bauernschmitt and R. Ahlrichs, Stability analysis for solutions of the closed shell Kohn–Sham equation, *J. Chem. Phys.*, 1996, **104**, 9047.
17 F. Furche and R. Ahlrichs, Adiabatic time-dependent density functional methods for excited state properties, *J. Chem. Phys.*, 2002, **117**, 7433.
18 A. Schäfer, C. Huber and R. Ahlrichs, Fully optimized contracted Gaussian basis sets of triple zeta valence quality for atoms Li to Kr, *J. Chem. Phys.*, 1994, **100**, 5829.
19 M. Reiher, D. Sellmann and B. A. Hess, Stabilization of diazene in Fe(II)-sulfur model complexes for nitrogenase activity. Part I. A new approach to the evaluation of intramolecular hydrogen bond energies, *Theor. Chem. Acc.*, 2001, **106**, 379–392.
20 J. R. D. McCormick, S. M. Fox, L. L. Smith, B. A. Bittler, J. Reichenthal, V. E. Origoni, W. H. Muller, R. Winterbottom and A. P. Doerschuk, Studies of the reversible epimerization occurring in the tetracycline family. The preparation, properties and proof of structure of some 4-*epi*-tetracyclines, *J. Am. Chem. Soc.*, 1957, **79**, 2849.
21 M. O. Schmitt and S. Schneider, Spectroscopic investigation of complexation between various tetracyclines and Mg^{2+} or Ca^{2+}, *PhysChemComm*, 2000, **3**(9), 42–55.
22 S. Schneider, Proton and metal ion binding of tetracyclines, in *Tetracyclines in Biology, Chemistry and Medicine*, ed. M. Nelson, W. Hillen and R. A. Greenwald, Birkhäuser Verlag, Basel, 2001, pp. 65–104.
23 L. A. Mitscher, *The Chemistry of the Tetracycline Antibiotics*, Marcel Dekker, New York, 1978.
24 H. A. Duarte, S. Carvalho, E. B. Paniago and A. M. Simas, Importance of tautomers in the chemical behavior of tetracyclines, *J. Pharm. Sci.*, 1999, **88**, 111–120.
25 H. Morrison G. Olack and C. Xiao, Photochemical and photophysical studies of tetracycline, *J. Am. Chem. Soc.*, 1991, **113**, 8110–8118.
26 A. Weller, Innermolekularer Protonenübergang im angeregten Zustand, *Z. Elektrochem.*, 1956, **60**, 1144–1177.
27 S. Schneider, G. Brehm, M. O. Schmitt, C. F. Leypold, M. Reiher, P. Matousek and M. Towrie, Kerr gated resonance Raman study of tetracyclines and their complexes with divalent metal ions, *Rutherford Appleton Lab., [Rep.] RAL*, 2001–2002, 100–103.
28 C. F. Leypold, M. Reiher, G. Brehm, M. O. Schmitt, S. Schneider, P. Matousek and M. Towrie, Tetracycline and Derivatives – Assignment of IR and Raman Spectra *via* DFT Calculations, *Phys. Chem. Chem. Phys.*, 2003, **5**, 1149–1157.
29 M. Kunz, Untersuchungen zu den Bindungszuständen des TetR(B) und deren Stuktur im Bereich der Aminosäuren 164–171, Ph.D. Thesis, Universität Erlangen-Nürnberg, Germany, 2000.
30 C. F. Leypold, Spektroskopische Untersuchungen von Tetrazyklinderivaten und deren Bindung in Tet Repressoren, Ph.D. Thesis, Universität Erlangen-Nürnberg, Germany, 2003.
31 C. F. Leypold, M. O. Schmitt, M. Reiher, S. Schneider, F. W. Frank, D. Sellmann and W. Bauer, Molecular geometry of tetracycline and doxycycline in the crystalline state and in solution investigated by X-ray, Raman, IR, and NMR spectroscopy, and *via* DFT calculations, manuscript in preparation.
32 A. Morimoto, T. Yatsuhashi, T. Shimada, S. Kumazaki, K. Yoshihara and H. Inoue, Molecular mechanism of the intermolecular hydrogen bond between 2-piperidinoanthraquinone and alcohol in the excited state: direct observation of the out-of-plane mode interaction with alcohol by transient absorption studies, *J. Phys. Chem. A*, 2001, **105**, 8840–8849.